Recent Optical Coherence Tomography Imaging of Vitreomacular Disorders

Manoharan Shunmugam, MBChB, MRCOphth and Tom H Williamson, MD, FRCS, FRCOphth, MBChB

Department of Ophthalmology, St Thomas' Hospital, London

Abstract

Optical coherence tomography (OCT) has become a ubiquitous and invaluable tool in the retinal clinic as it provides the examiner with a 2D cross-section of the retina; newer machines are also able to reconstruct 3D images. The greater detail afforded by OCT scanning enhances diagnostic capabilities and advances vitreoretinal research. It has proved very useful in surgical planning and provides fine anatomical retinal detail, which can aid post-operative prognostication in certain vitreoretinal disorders. OCT operates on the same physical principles as an ultrasound scan, except it uses light as the carrier signal. First-generation OCTs are capable of resolutions only between 10 and 20µm. Second-generation OCTs improved this to 5–6µm. We await the commercial availability of third-generation and full-field OCTs, which yield resolutions as low as 1–3µm.

Keywords

Retinal diseases, diagnostic imaging, tomography, optical coherence

Disclosure: The authors have no conflicts of interest to declare.
Acknowledgment: The authors would like to thank Dr Lucia Pelosini for providing the various optical coherence tomography images in this article.
Received: September 24, 2009 **Accepted:** July 7, 2010 **Citation:** *US Ophthalmic Review*, 2011;4(1):17–22 *DOI: 10.17925/USOR.2011.04.01.17*
Correspondence: Manoharan Shunmugam, MBChB, MRCOphth, Department of Ophthalmology, St Thomas' Hospital, Westminster Bridge Road, London, SE1 7EH, UK.
E: manoshun@doctors.org.uk

Optical coherence tomography (OCT), first developed for ophthalmic imaging in the 1990s,[1] has become a ubiquitous and invaluable tool in the retinal clinic. While it will never replace stereoscopic biomicroscopy, it has demonstrated clear advantages. Adjunctive OCT scanning objectively provides the examiner with 2D cross-sections of the retina, while newer machines are able to reconstruct 3D images. Adequate clinical examination of the vitreoretinal interface requires a fundus contact lens and suffers from inter-observer variation, subjective documentation, and missed pathology. From a patient's perspective, contact lens examinations can be uncomfortable and distressing. The greater detail afforded by OCT scanning also enhances the clinician's ability to clinch diagnoses and further vitreoretinal research.

The first-generation (time-domain [TD]) OCTs were capable of resolutions only between 10 and 20µm. Second-generation (spectral-domain [SD]) OCTs have a resolution of 5–6µm. We eagerly await the commercial availability of third-generation (swept-source [SS]) OCT, which yields resolutions as low as 1–3µm. These devices have already transformed the field of retinal research, allowing visualization and measurement of retinal vascular blood flow. Full-field OCTs are still not available for clinical use, but the promise of single-micron resolution is not far off.

Optical Coherence Tomography Imaging

Time-domain Optical Coherence Tomography

Conceptually, OCT operates on the same physical principles as an ultrasound scan, except it uses light as the carrier signal. As such, the spatial resolution of an OCT is much higher than a conventional 10–20MHz ultrasound as a result of the naturally shorter wavelength of light. The source of light in an OCT is produced by a super-luminescent diode, femtosecond laser or, of late, white light.[2]

Simplistically, the OCT works by splitting a beam of light into two arms: a reference arm and a sampling arm. First-generation OCTs are TD-OCT, so named because the length of the reference arm is varied with time in order to correlate with the back-reflected sample arm. This is achieved with the use of an adjustable mirror of known distance within the device. The sample arm is focused onto the retina with the use of an in-built 78D lens. The sample beam is reflected off the structures in the eye and is re-combined with the reference beam by using a Michaelson interferometer within the unit. A single cycle of this process yields one A-scan. This single scan comprises data on the distance the sample arm has travelled and the back-reflectance and back-scatter of the beam. Tissue layers at varying depths and optical characteristics produce differing reflective intensities. As in an ultrasound scan, in order to produce a B-scan image, multiple A-scans are obtained in rapid succession across the area of interest. Software combines this information to produce a 2D image either in greyscale or with arbitrary false-coloring. The result is a cross-sectional scan, a reconstructed 3D topographical image, quantitative thickness measurements or, more recently, z-plane or coronal scans.[2]

Frequency-domain Optical Coherence Tomography

Frequency-domain OCT (FD-OCT) operates on a slightly different principle. Instead of matching reference and sample arm lengths, the axial scan is

Table 1: Specification Comparison of a Few Commercially Available Optical Coherence Tomography Scanners

Device	Manufacturer	Technology	Signal Wavelength (nm)	Scan Speed (A-scans)	Axial Resolution (µm)	Transverse Resolution (µm)	Scanning Field	Macular Depth Range (mm)	Additional Features
STRATUS OCT™	Carl Zeiss Meditec, Inc.	TD-OCT	820 (NIR) SLD	400	≤10	20	26x20.5º	2	
RTVue-100	Optovue	SD-OCT	840 (NIR)	26,000	5	15	32x23º	2	
Cirrus™ HD-OCT	Carl Zeiss Meditec, Inc.	SD-OCT	840 SLD	27,000	5	15	36x30º	2	Line scanning, ophthalmoscope
SPECTRALIS® OCT	Heidelberg Engineering, Inc.	SD-OCT	820 laser diode and 870 SLD	40,000	3.9	14	55º	1.8	Active eye tracking
SPECTRALIS® OCTPLUS	Heidelberg Engineering, Inc.	SD-OCT	820 laser diode and 870 SLD	40,000	3.9	14	55–150º	1.8	Active eye tracking, peripheral and wide-field OCT
3D OCT-1000 Mark II	Topcon Medical Systems	SD-OCT	840 SLD	18,000	5–6	≤20	8.2x3mm (45º)	2.3	Colour non-mydriatic retinal camera
SOCT Copernicus HR	Optopol Technology	SD-OCT	850 SLD	52,000	3	12–18	10mm	2	
Spectral OCT/SLO	OPKO Instruments/OTI	SD-OCT	830 SLD	27,000	5–6	20	29º	2	Registration with SLO, microperimetry
Bioptigen SDOCT	Bioptigen	SD-OCT	820 (NIR)	17,000	4.5	15	50º	2	Handheld OCT (60º)

NIR = near infrared; OCT = optical coherence tomography; D-OCT = spectral-domain optical coherence tomography; SLD = superluminescent diode; SLO = scanning laser ophthalmoscope; TD-OCT = time-domain optical coherence tomography.

calculated by Fourier-transformation of the acquired spectral interference fringes generated by the interaction of the reference and sample arms. Therefore, the reference arm in an FD-OCT does not have to move, allowing dramatically quicker scan acquisition speeds. SD-OCT, also known as Fourier-domain OCT, is based on the underlying principle of FD-OCT, but SD-OCT is able to extract more information in a single scan as it distributes several optical frequencies onto a detector stripe.[3] Time-encoded FD-OCT, also known as SS-OCT, is again based on FD-OCT. However, unlike Fourier-domain OCT, which emits multiple optical frequencies all at once, the SS-OCT emits multiple frequencies in single successive steps. At present, SS-OCT is not commercially available, but it has shown promise in recent studies that have demonstrated significantly improved resolution and image penetration for imaging structures and pathology deep in the retina because it operates in the 1,050nm wavelength range.[4,5] Each mode of frequency encoding has its advantages and limitations, but a detailed analysis is beyond the scope of this article.

Full-field Optical Coherence Tomography

The latest-generation OCT is the full-field OCT (FF-OCT), another version of the TD-OCT, and uses a broadband (white) light source instead of a laser or super-luminescent diode.[2] Also known as T-scan (transverse) OCT or *en face* OCT, it acquires tomographic data by acquiring multiple coronal scans instead of the usual axial scans (A-scans) of the previously described TD-OCT.[6] It should be noted that SS-OCT is also capable of this scanning scheme.[7] The advantage of this method is that it is possible to generate not only B-scans but also C-scans (coronal) alongside a simultaneous, conventional fundus image (coronal plane). This presents a unique opportunity for developers to combine other imaging modalities with OCT, as the focusing requirements (in z-plane) are relaxed and dynamic focusing is possible. The downside is that image acquisition times are, at present, significantly longer, taking at least a few seconds compared with SD-OCT, which is able to acquire a full scan in under one second.[8] Like a magnetic resonance imaging (MRI) scan, full data acquisition is required before a coronal scan can be produced with the FF-OCT due to the concavity of the fundus.[6]

Scanning Modes

As briefly mentioned above, actually obtaining a scan requires sequential scanning in the form of multiple A-scans for TD-OCT and SD-OCT, and C-scans for FF-OCT. The volume of information obtained can be measured in volumetric pixels (voxels).[7] Increasing the number of voxels captured can be achieved by either increasing the scanning frequency rate or using multidetector arrays, or both.[3,7] Commercially available SD-OCT scanners became available in early 2006, and most have imaging speeds of 25,000 axial scans per second with an axial resolution of between 5 and 7µm (see *Table 1*). Technological optimization of these variables has produced OCT scanners that achieve up to 250,000 axial scans per second while maintaining axial resolution at 8–9µm, thus yielding more than 100 megavoxels.[7] Clinically, this translates into a high-resolution macular scan in 1.3 seconds or even the potential to measure blood-flow velocities in vessels as narrow as 13.64µm.[9,10] Higher scanning speeds are less likely to suffer from motion artefact.[11] Signal strength is the measure of the amount of reflected light received by the scanner. It is graded to serve as a proxy measure of scan quality. A signal strength of at least seven should be aimed for in order to obtain consistently accurate results.[12,13] High scan rates can reduce signal strengths to below this.[7]

Numerous software-controlled scanning protocols translate voxel datasets into clinically representative images. Post-scan software processing also determines surface segmentations such as the internal limiting membrane (ILM) and retinal pigment epithelium (RPE), among others, and assigns a false color to each layer depending on the signal reflectance (see *Figure 1*). However, greyscale and proportion-corrected OCT images reveal a finer gradation of signal reflectance and can be used to demonstrate additional information not present in false-color

images.[14] Software outlining of the ILM is necessary for the calculation of retinal thickness, however, it has been shown to be inaccurate in up to 19% of scans.[15] New algorithms are being constantly developed to overcome these shortfalls.[15–17] In a direct comparison of TD-OCT and FD-OCT, the measurements obtained were comparable. Results depended more on the algorithm used than the hardware, emphasizing the need for robust software.[18] It is also pertinent that the clinician always double-checks these analyses as artefacts exist (43.2% in one study, with 30% requiring manual remeasurement due to spurious central point thickness [CPT]).[19]

Clinical Applications

General Ophthalmic Applications

Following its introduction for retinal and coronary imaging in the 1990s, OCT has diversified to other medical fields as varied as hair-growth analysis for discovering steroid-doping athletes.[20] In ophthalmology, OCT is used to image the anterior segment,[21,22] retina and, with recent technological developments, the choroid in greater detail than before.[23] OCT is well-established in glaucoma practice, allowing the quantification of nerve fiber loss and disc morphology.[24]

Macular Topography

OCT provides an objective quantification of retinal structures, unlike fundus fluorescein angiography, autofluorescence or retinal photography. Additionally, the rapid, non-contact, non-invasive nature of OCT scanning lends itself to the busy vitreoretinal clinic. Obtaining an OCT image requires mydriasis to ensure an artefact-free scan. Non-mydriatic scanning is possible but may result in vignetting of the macular scan as the edges of the sample beam are clipped by the pupillary margin. If it is not possible to dilate the patient, scanning in a dark environment would reduce this phenomenon as the vast majority of OCT scanners use near-infrared light, which does not induce pupillary constriction. The macula is visualized on the monitor and the area of interest is aligned with the aid of fixation targets. It is useful to ensure the patient blinks several times prior to acquiring the scan to ensure an even tear film. Even the presence of contact lenses can affect retinal nerve fiber layer thickness measurements.[25] Dense media opacities will degrade image quality, although OCT is able to quite effectively penetrate most cataracts, asteroid hyalosis and vitritis. Mathematical models have been developed to improve the quality of these degraded images,[26] however, the experienced examiner is usually still able to discern sufficient detail in most cases.

Central retinal thickness was compared between six commercially available OCT scanners in a study involving healthy eyes. A variation of between 0.45 and 3.33% was found. The discrepancies were explained by the slightly different segmentation algorithms employed by each device.[27] In effect, this means that the line the software uses to determine the outer retinal boundary differs, so different OCT systems should not be used interchangeably.[27,28]

On the fast macular thickness map protocol with TD-OCT scanning,[6] radial sampling scans of the macula are acquired and a macular topographical color-coded map of the macula is produced. The software interpolates adjacent thickness values in the interspersing macular areas that lie between the six radial scans. Clinicians should therefore be aware of small lesions suspected to lie within these areas, as they may not be picked up with this protocol. This is not an issue with the newer SD-OCT, which acquires a faster series of high-resolution images.[11]

Figure 1: False-color Optical Coherence Tomography Image Showing a Pigment Epithelial Detachment

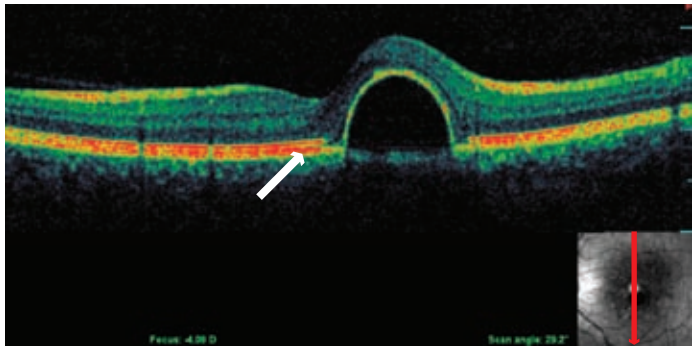

Intact area of outer red line (arrow) represents reflection from the retinal pigment epithelium, Bruch's membrane and inner choroidal complex.

Figure 2: High-resolution Optical Coherence Tomography B-scan Image of the Normal Human Macula

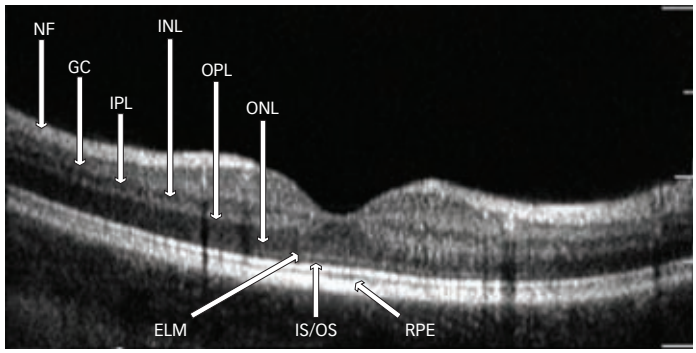

ELM = external limiting membrane; GC = ganglion cell layer; IPL = inner plexiform layer; INL = inner nuclear layer; IS/OS = photoreceptor inner and outer segment junction; NF = nerve fiber layer; ONL = outer nuclear layer; OPL = outer plexiform layer; RPE = retinal pigment epithelium and inner choroidal layers.

With higher-resolution scanning, a cross-sectional B-scan can reveal most layers within the neurosensory retina (see *Figure 2*).[29] A few histologic studies have correlated the appearance of the OCT with histologic sections of human and animal retinas.[30,31] Further studies have correlated the segmentation (bands) on an OCT with retinal layers by surgical sequential ablation of these layers.[32,33] The outer red line (ORL) is frequently assumed to represent the RPE alone, but in actuality corresponds to the highly reflective chorio-retinal complex as a whole (see *Figure 1*). The predominant contribution to the ORL is by the Bruch's membrane and inner choroid, with a smaller contribution by the RPE.[33] Of particular interest is the band correlating to the junction of the inner and outer segment (IS/OS) of the photoreceptors (see *Figure 2*). This is better visualized as a 'red line' just inside the ORL on the higher-resolution SD-OCT. The IS/OS band is a high-reflectance signal at this junction resulting from the abrupt change in the refractive index stemming from the highly organized stacks of membranous disks in the photoreceptor outer segments.[29] OCT changes in this area have been studied in a number of conditions, and visual acuity (VA) has been

Figure 3: Loss of Photoreceptor Inner and Outer Segment, with Intact External Limiting Membrane (arrow) on B-scan Optical Coherence Tomography Image of Cystoid Macular Edema

Figure 4: Fundus Photograph (A) and B-scan Optical Coherence Tomograph of an Epiretinal Membrane (B)

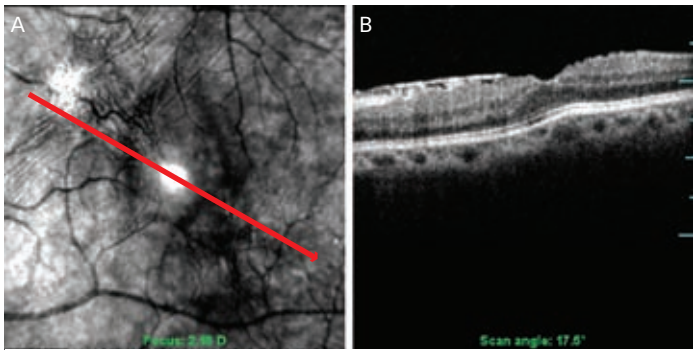

A: Fundus photograph of a macular epiretinal membrane (ERM) with indication of B-scan optical coherence tomography (OCT) section (red arrow); B: B-scan OCT of ERM revealing highly reflective ERM with underlying retinal folds but intact photoreceptor inner and outer segment (IS/OS) junction and external limiting membrane (ELM).

significantly correlated with OCT detection of the IS/OS junction in retinitis pigmentosa,[34] macula-off retinal detachments,[35] full-thickness macular holes,[36–38] central serous chorioretinopathy,[39] age-related macular degeneration (AMD)[40] and macular edema associated with branch retinal vein occlusions.[41,42] As IS/OS disruption (see *Figure 3*) reflects VA, the external limiting membrane (ELM) appears to show prognostic promise.[35] In a series of consecutive retinal detachments (RDs), IS/OS disruption was observed in macula-off eyes. As predicted, post-operative VA was significantly correlated with IS/OS integrity. None of the eyes with pre-operative disruption of ELM and IS/OS regained post-operative IS/OS integrity. By contrast, seven of the 11 eyes that had intact ELM on OCT pre-operatively regained the IS/OS junction during follow-up.[35]

Vitreomacular Traction Syndrome

Vitreomacular traction syndrome (VMTS) is a condition in which the vitreous is separated from the peripheral fundus but remains adherent in the macular area. OCT is instrumental in diagnosing and monitoring progression, or in some cases confirming resolution. Prior to the availability of OCT, most cases were diagnosed with careful contact lens fundoscopy. More recently, some surgeons have proposed utilizing OCT as a pre-operative surgical planning tool to guide posterior hyaloid membrane peeling in VMTS by locating the area of greatest separation of the posterior hyaloid from the macula.[43]

A novel method of vitreoretinal interface imaging combines FF-OCT with simultaneous scanning laser ophthalmoscopy (SLO) to produce a coronal image of the retina, which provides a broader overview of vitreoretinal attachment.[44] Second, as the SLO image is co-registered with the OCT, it is easier to orientate and localize pathology. A more anatomical perspective of the posterior hyaloid obtained in this manner will also allow the ophthalmologist to better assess the severity and concurrence of other vitreoretinal disorders, such as epiretinal membranes (ERMs), which frequently co-exist with VMTS.[45]

Age-related Macular Degeneration

Vitreomacular traction has been associated with neovascular AMD, however, Lee and colleagues[46] reported that by comparing eyes with wet AMD versus contralateral normal eyes of the same patient, no statistically significant differences in vitreomacular adhesion were found with respect to choroidal neovascular membrane (CNVM) location or type.[46] Nevertheless, OCT is invaluable in the initial assessment of AMD either when FFA is not available or as an adjunct to FFA. As a screening test, it is able to detect the presence and location of fluid or atrophy, thus reducing the need for unnecessary FFAs. With the increase in anti-vascular endothelial growth factor (anti-VEGF) treatments, OCT has become an indispensible tool in the screening and monitoring of CNV presence and progression or response to treatment, especially since it can demonstrate subtle disease activity prior to symptomatic or biomicroscopic changes.[47] In the past, this was the sole remit of the resource-consuming and more invasive FFA, which is now mainly used for diagnostic confirmation and typing in most units in the UK. Furthermore, OCT provides objective documentation of progress compared with FFA, which has been reported to have comparatively poorer inter-observer agreement, especially following treatment.[48–50] A study assessing the sensitivity of TD-OCT against SD-OCT in the detection of subretinal and intraretinal fluid as a proxy for CNV activity following intravitreal ranibizumab injection found that 3D SD-OCT had the highest detection rates, followed by SD-OCT linear scans and, lastly, TD-OCT.[28] A good indicator of visual outcomes after anti-VEGF therapy is the preservation of the IS/OS junctions of the photoreceptors (see *Figures 2* and *3*).[40] Sayanagi and colleagues used four different SD-OCT machines to evaluate the status of the IS/OS in 23 eyes of 22 AMD patients who had received a mean of 5.4 (SD=3.2) anti-VEGF injections over an average of 10.4 months (SD=8) prior to imaging. There was a significant difference in detection of the IS/OS between the AMD patients and the eight healthy eyes. Statistically, eyes with detected IS/OS had better best corrected VA (BCVA) on the day of imaging and significantly improved BCVA since the start of anti-VEGF treatment.[40]

Reduced reflectance from the IS/OS has also been demonstrated in areas of drusen. This phenomenon can be explained by either photoreceptor damage or elevatory disruption of the vertically orientated photoreceptors by the underlying drusen.[51,52] Further studies with larger populations are required to determine the clinical significance of this finding, which may in the future provide clinicians with valuable prognostic information in the management of wet and dry AMD alike.

New SS-OCT technology, with its improved axial beam penetration, allows for improved structural delineation and qualitative evaluation of lesions located beneath the RPE.[4] It has allowed clear demonstration of polypoidal choroidal vasculopathy (PCV) lesions *in vivo*, pinpointing its location

between displaced RPE and the outer part of Bruch's membrane,[53] which is in agreement with histopathological studies.[54] Identification and differentiation of such lesions from wet AMD is important, as treatment regimes differ, with PCV responding to photodynamic therapy.[55,56]

Epiretinal Membranes

ERMs are caused by glial proliferation on the surface of the macula and can cause varying degrees of vascular distortion, or even macular edema. OCT displays this membrane as a thin, smooth, hyper-reflective line along the surface of the retina (see *Figure 4*). Careful evaluation of the OCT can reveal the extent of ERM adherence to the underlying retina, the character of which correlates with the pathogenesis.[57] Focal attachments of the highly reflective ERM to the less reflective inner retinal surface can sometimes be easier to discern than global ERM adherence, which can make the ERM indistinct from the ILM. Focal adhesions are more commonly seen in secondary ERMs, while global adhesion is more prevalent in idiopathic ERMs.[57] ERMs are usually smooth, but can produce retinal folds, inner retinal irregularity and diffuse retinal thickening, which can be fully appreciated on 3D OCT rendering.[58] 3D scanning could also aid surgical planning as it reveals the manner and direction of ERM traction on the retina.[58]

Some studies have found a correlation between VA and retinal thickness in eyes with idiopathic ERMs;[57] however, this has not been found in other studies.[59,60] Higher-resolution OCTs have improved pre-operative ERM evaluation[60] (see *Figure 4*) and have demonstrated that central foveal thickness (CFT) correlates with both pre-operative VA and IS/OS abnormalities.[61,62] Suh et al. also found that patients with intact IS/OS had better BCVA post-operatively. By grading the status of the IS/OS (see *Figures 2* and *3*) as present, absent or abnormal, Mitamura and colleagues found that logMAR BCVA correlated with both pre-operative CFT and IS/OS grades. However, at three and six months post-operatively, BCVA correlated only with the status of the IS/OS and not CFT. The percentage of eyes with a normal IS/OS gradually increased post-operatively.

Macular Holes

Full-thickness macular holes (FTMHs) are easily confused clinically with lamellar and pseudoholes. Accurate diagnosis is essential as management differs greatly. In one study, almost two-thirds of cases (63%) found to have a lamellar macular hole (LMH) on OCT were initially incorrectly diagnosed as either a FTMH, ERM or macular pseudohole on biomicroscopy.[63] OCT grading of FTMH status can guide the urgency of treatment.

LMHs are now primarily an OCT-based diagnosis as biomicroscopy provides insufficient resolution to detect residual outer retina, foveal photoreceptors, or intraretinal split,[63] the presence of which explains the relatively preserved vision in this group of patients. The almost constant finding of an ERM in the presence of LMH[63,64] could shed light on its evolution. Gass,[65] along with a few other authors,[66–68] proposed that LMHs were a result of an abortive process of a FTMH.

Gass also described the formation of LMH following chronic cystoid macular edema (CME).[65] An observational case series reporting four patients followed up with OCT confirmed that the occurrence of an LMH following refractory (diabetic) CMO is most likely due to the rupture of the inner wall of the thinned, cystic spaces. None of the four patients experienced any change in VA despite remarkable anatomical reduction in foveal thickness (from a mean of 509 to 166µm). In all cases, high-resolution OCT revealed that the outer retinal layer remained, with at least intermittently recognisable IS/OS.[69]

FTMHs have been extensively investigated with the use of OCT; the clinical features associated with improved visual prognosis are well-known and include better VA on presentation, duration of symptoms and hole diameter.[70–72] Post-operatively, a few studies have revealed that the presence of an intact IS/OS is an important indicator of visual recovery, with the number of patients with detectable IS/OS increasing over time following FTMH repair.[37] The post-operative status of the IS/OS line on OCT correlates well with VA,[36–38] with a significant correlation between the post-operative presence of the IS/OS and the pre-operative duration of symptoms.

Post-operative IS/OS line 'healing' appears to occur at differing rates,[36,37] and it is still unknown how some patients continually show gradual visual recovery years after FTMH repair. There are probably numerous other prognostic determinants yet to be discovered as, histologically, photoreceptors are reported to remain intact in the fluid cuff of a FTMH[73] and, if viable, could possibly regenerate inner and outer segments.[74] These findings infer photoreceptor recovery and provide signs of anatomical success on an almost histological scale.

Summary and Future Directions

OCT has proved to be a powerful and versatile medical tool. It provides a non-contact method of objectively quantifying many conditions affecting the retina and has revolutionized the manner in which certain vitreomacular conditions are diagnosed and managed. It has shown promise as a tool for surgical planning and provides fine anatomical detail of the retina, which can aid post-operative prognostication. Newer-generation OCTs have already been widely used for research purposes and we eagerly await their commercial availability. ■

1. Huang D, Swanson EA, Lin CP, et al., Optical coherence tomography, *Science*, 1991;254(5035):1178–81.
2. Sacchet D, Moreau J, Georges P, Dubois A, Simultaneous dual-band ultra-high resolution full-field optical coherence tomography, *Opt Express*, 2008;16(24):19434–46.
3. Bourquin S, Seitz P, Salathe RP, Optical coherence topography based on a two-dimensional smart detector array, *Opt Lett*, 2001;26(8):512–4.
4. Yasuno Y, Miura M, Kawana K, et al., Visualization of sub-retinal pigment epithelium morphologies of exudative macular diseases by high-penetration optical coherence tomography, *Invest Ophthalmol Vis Sci*, 2009;50(1):405–13.
5. Srinivasan VJ, Adler DC, Chen Y, et al., Ultrahigh-speed optical coherence tomography for three-dimensional and en face imaging of the retina and optic nerve head, *Invest Ophthalmol Vis Sci*, 2008;49(11):5103–10.
6. Rosen RB, Hathaway M, Rogers J, et al., Multidimensional en-face OCT imaging of the retina, *Opt Express*, 2009;17(5):4112–33.
7. Potsaid B, Gorczynska I, Srinivasan VJ, et al., Ultrahigh speed spectral / Fourier domain OCT ophthalmic imaging at 70,000 to 312,500 axial scans per second, *Opt Express*, 2008;16(19):15149–69.
8. Huber R, Adler DC, Srinivasan VJ, Fujimoto JG, Fourier domain mode locking at 1050 nm for ultra-high-speed optical coherence tomography of the human retina at 236,000 axial scans per second, *Opt Lett*, 2007;32(14):2049–51.
9. Wang RK, An L, Doppler optical micro-angiography for volumetric imaging of vascular perfusion in vivo, *Opt Express*, 2009;17(11):8926–40.
10. Tao YK, Kennedy KM, Izatt JA, Velocity-resolved 3D retinal microvessel imaging using single-pass flow imaging spectral domain optical coherence tomography, *Opt Express*, 2009;17(5):4177–88.
11. Srinivasan VJ, Wojtkowski M, Witkin AJ, et al., High-definition and 3-dimensional imaging of macular pathologies with high-speed ultrahigh-resolution optical coherence tomography, *Ophthalmology*, 2006;113(11):2054, e1–14.
12. Wu Z, Vazeen M, Varma R, Chopra V, et al., Factors associated with variability in retinal nerve fiber layer thickness measurements obtained by optical coherence tomography, *Ophthalmology*, 2007;114(8):1505–12.
13. Wu Z, Huang J, Dustin L, Sadda SR, Signal strength is an important determinant of accuracy of nerve fiber layer thickness measurement by optical coherence tomography,

J Glaucoma, 2009;18(3):213–6.
14. Ishikawa H, Gurses-Ozden R, Hoh ST, et al., Grayscale and proportion-corrected optical coherence tomography images, *Ophthalmic Surg Lasers*, 2000;31(3):223–8.
15. Haeker M, Abramoff M, Kardon R, Sonka M, Segmentation of the surfaces of the retinal layer from OCT images, *Med Image Comput Assist Interv Int*, 2006;9(Pt 1):800–7.
16. Garvin M, Abramoff M, Wu X, et al., Automated 3-D Intraretinal Layer Segmentation of Macular Spectral-Domain Optical Coherence Tomography Images, *IEEE Trans Med Imaging*, 2009;28(9):1436–47.
17. Sadda SR, Joeres S, Wu Z, et al., Error correction and quantitative subanalysis of optical coherence tomography data using computer-assisted grading, *Invest Ophthalmol Vis Sci*, 2007;48(2):839–48.
18. Hood DC, Raza AS, Kay KY, et al., A comparison of retinal nerve fiber layer (RNFL) thickness obtained with frequency and time domain optical coherence tomography (OCT), *Opt Express*, 2009;17(5):3997–4003.
19. Domalpally A, Danis RP, Zhang B, et al., Quality issues in interpretation of optical coherence tomograms in macular diseases, *Retina*, 2009;29(6):775–81.
20. Lademann J, Shevtsova J, Patzelt A, et al., Optical coherent tomography for in vivo determination of changes in hair cross section and diameter during treatment with glucocorticosteroids—a simple method to screen for doping substances?, *Skin Pharmacol Physiol*, 2008;21(6):312–7.
21. Izatt JA, Hee MR, Swanson EA, et al., Micrometer-scale resolution imaging of the anterior eye in vivo with optical coherence tomography, *Arch Ophthalmol*, 1994;112(12):1584–9.
22. Lei K, Wang N, Wang L, Wang B, Morphological changes of the anterior segment after laser peripheral iridotomy in primary angle closure, *Eye*, 2009;23(2):345–50.
23. Margolis R, Spaide RF, A pilot study of enhanced depth imaging optical coherence tomography of the choroid in normal eyes, *Am J Ophthalmol*, 2009;147(5):811–5.
24. Paunescu LA, Schuman JS, Price LL, et al., Reproducibility of nerve fiber thickness, macular thickness, and optic nerve head measurements using Stratus OCT, *Invest Ophthalmol Vis Sci*, 2004;45(6):1716–24.
25. Youm DJ, Kim JM, Park KH, Choi CY, The effect of soft contact lenses during the measurement of retinal nerve fiber layer thickness using optical coherence tomography, *Curr Eye Res*, 2009;34(1):78–83.
26. Tappeiner C, Barthelmes D, Abegg MH, et al., Impact of optic media opacities and image compression on quantitative analysis of optical coherence tomography, *Invest Ophthalmol Vis Sci*, 2008;49(4):1609–14.
27. Wolf-Schnurrbusch UE, Ceklic L, Brinkmann CK, et al., Macular thickness measurements in healthy eyes using six different optical coherence tomography instruments, *Invest Ophthalmol Vis Sci*, 2009;50(7):3432–7.
28. Sayanagi K, Sharma S, Yamamoto T, Kaiser PK, Comparison of spectral-domain versus time-domain optical coherence tomography in management of age-related macular degeneration with ranibizumab, *Ophthalmology*, 2009;116(5):947–55.
29. Chan A, Duker JS, Ishikawa H, et al., Quantification of photoreceptor layer thickness in normal eyes using optical coherence tomography, *Retina*, 2006;26(6):655–60.
30. Hoang QV, Linsenmeier RA, Chung CK, Curcio CA, Photoreceptor inner segments in monkey and human retina: mitochondrial density, optics, and regional variation, *Vis Neurosci*, 2002;19(4):395–407.
31. Gloesmann M, Hermann B, Schubert C, et al., Histologic correlation of pig retina radial stratification with ultrahigh-resolution optical coherence tomography, *Invest Ophthalmol Vis Sci*, 2003;44(4):1696–703.
32. Chauhan DS, Marshall J, The interpretation of optical coherence tomography images of the retina, *Invest Ophthalmol Vis Sci*, 1999;40(10):2332–42.
33. Ghazi NG, Dibernardo C, Ying HS, et al., Optical coherence tomography of enucleated human eye specimens with histological correlation: origin of the outer 'red line', *Am J Ophthalmol*, 2006;141(4):719–26.
34. Aizawa S, Mitamura Y, Baba T, et al., Correlation between visual function and photoreceptor inner/outer segment junction in patients with retinitis pigmentosa, *Eye*, 2009;23(2):304–8.
35. Wakabayashi T, Oshima Y, Fujimoto H, et al., Foveal microstructure and visual acuity after retinal detachment repair: imaging analysis by Fourier-domain optical coherence tomography, *Ophthalmology*, 2009;116(3):519–28.
36. Sano M, Shimoda Y, Hashimoto H, Kishi S, Restored photoreceptor outer segment and visual recovery after macular hole closure, *Am J Ophthalmol*, 2009;147(2):313–8 e1.
37. Baba T, Yamamoto S, Arai M, et al., Correlation of visual recovery and presence of photoreceptor inner/outer segment junction in optical coherence images after successful macular hole repair, *Retina*, 2008;28(3):453–8.
38. Inoue M, Watanabe Y, Arakawa A, et al., Spectral-domain optical coherence tomography images of inner/outer segment junctions and macular hole surgery outcomes, *Graefes Arch Clin Exp Ophthalmol*, 2009;247(3):325–30.
39. Piccolino FC, de la Longrais RR, et al., The foveal photoreceptor layer and visual acuity loss in central serous chorioretinopathy, *Am J Ophthalmol*, 2005;139(1):87–99.
40. Sayanagi K, Sharma S, Kaiser PK, Photoreceptor status after antivascular endothelial growth factor therapy in exudative age-related macular degeneration, *Br J Ophthalmol*, 2009;93(5):622–6.
41. Ota M, Tsujikawa A, Murakami T, et al., Foveal photoreceptor layer in eyes with persistent cystoid macular edema associated with branch retinal vein occlusion, *Am J Ophthalmol*, 2008;145(2):273–80.
42. Murakami T, Tsujikawa A, Ohta M, et al., Photoreceptor status after resolved macular edema in branch retinal vein occlusion treated with tissue plasminogen activator, *Am J Ophthalmol*, 2007;143(1):171–3.
43. Chung EJ, Lew YJ, Lee H, Koh HJ, OCT-guided hyaloid release for vitreomacular traction syndrome, *Korean J Ophthalmol*, 2008;22(3):169–73.
44. Tammewar AM, Bartsch DU, Kozak I, et al., Imaging vitreomacular interface abnormalities in the coronal plane by simultaneous combined scanning laser and optical coherence tomography, *Br J Ophthalmol*, 2009;93(3):366–72.
45. Koizumi H, Spaide RF, Fisher YL, et al., Three-dimensional evaluation of vitreomacular traction and epiretinal membrane using spectral-domain optical coherence tomography, *Am J Ophthalmol*, 2008;145(3):509–17.
46. Lee SJ, Lee CS, Koh HJ, Posterior vitreomacular adhesion and risk of exudative age-related macular degeneration: paired eye study, *Am J Ophthalmol*, 2009;147(4):621–6 e1.
47. Brown DM, Regillo CD, Anti-VEGF agents in the treatment of neovascular age-related macular degeneration: applying clinical trial results to the treatment of everyday patients, *Am J Ophthalmol*, 2007;144(4):627–37.
48. van Velthoven ME, de Smet MD, Schlingemann RO, et al., Added value of OCT in evaluating the presence of leakage in patients with age-related macular degeneration treated with PDT, *Graefes Arch Clin Exp Ophthalmol*, 2006;244(9):1119–23.
49. Friedman SM, Margo CE, Choroidal neovascular membranes: reproducibility of angiographic interpretation, *Am J Ophthalmol*, 2000;130(6):839–41.
50. Holz FG, Jorzik J, Schutt F, et al., Agreement among ophthalmologists in evaluating fluorescein angiograms in patients with neovascular age-related macular degeneration for photodynamic therapy eligibility (FLAP-study), *Ophthalmology*, 2003;110(2):400–5.
51. Gorczynska I, Srinivasan VJ, Vuong LN, et al., Projection OCT fundus imaging for visualising outer retinal pathology in non-exudative age-related macular degeneration, *Br J Ophthalmol*, 2009;93(5):603–9.
52. Yi K, Mujat M, Park BH, et al., Spectral domain optical coherence tomography for quantitative evaluation of drusen and associated structural changes in non-neovascular age-related macular degeneration, *Br J Ophthalmol*, 2009;93(2):176–81.
53. Ojima Y, Hangai M, Sakamoto A, et al., Improved visualization of polypoidal choroidal vasculopathy lesions using spectral-domain optical coherence tomography, *Retina*, 2009;29(1):52–9.
54. Lafaut BA, Aisenbrey S, Van den Broecke C, et al., Polypoidal choroidal vasculopathy pattern in age-related macular degeneration: a clinicopathologic correlation, *Retina*, 2000;20(6):650–4.
55. Shima C, Gomi F, Sawa M, et al., One-year results of combined photodynamic therapy and intravitreal bevacizumab injection for retinal pigment epithelial detachment secondary to age-related macular degeneration, *Graefes Arch Clin Exp Ophthalmol*, 2009;247(7):899–906.
56. Gomi F, Tano Y, Polypoidal choroidal vasculopathy and treatments, *Curr Opin Ophthalmol*, 2008;19(3):208–12.
57. Mori K, Gehlbach PL, Sano A, et al., Comparison of epiretinal membranes of differing pathogenesis using optical coherence tomography, *Retina*, 2004;24(1):57–62.
58. Legarreta JE, Gregori G, Knighton RW, et al., Three-dimensional spectral-domain optical coherence tomography images of the retina in the presence of epiretinal membranes, *Am J Ophthalmol*, 2008;145(6):1023–30.
59. Michalewski J, Michalewska Z, Cisiecki S, Nawrocki J, Morphologically functional correlations of macular pathology connected with epiretinal membrane formation in spectral optical coherence tomography (SOCT), *Graefes Arch Clin Exp Ophthalmol*, 2007;245(11):1623–31.
60. Massin P, Allouch C, Haouchine B, et al., Optical coherence tomography of idiopathic macular epiretinal membranes before and after surgery, *Am J Ophthalmol*, 2000;130(6):732–9.
61. Mitamura Y, Hirano K, Baba T, Yamamoto S, Correlation of visual recovery with presence of photoreceptor inner/outer segment junction in optical coherence images after epiretinal membrane surgery, *Br J Ophthalmol*, 2009;93(2):171–5.
62. Suh MH, Seo JM, Park KH, Yu HG, Associations between macular findings by optical coherence tomography and visual outcomes after epiretinal membrane removal, *Am J Ophthalmol*, 2009;147(3):473–80 e3.
63. Witkin AJ, Ko TH, Fujimoto JG, et al., Redefining lamellar holes and the vitreomacular interface: an ultra-high-resolution optical coherence tomography study, *Ophthalmology*, 2006;113(3):388–97.
64. Garretson BR, Pollack JS, Ruby AJ, et al., Vitrectomy for a symptomatic lamellar macular hole, *Ophthalmology*, 2008;115(5):884–6 e1.
65. Gass JD, Lamellar macular hole: a complication of cystoid macular edema after cataract extraction, *Arch Ophthalmol*, 1976;94(5):793–800.
66. Takahashi H, Kishi S, Tomographic features of a lamellar macular hole formation and a lamellar hole that progressed to a full-thickness macular hole, *Am J Ophthalmol*, 2000;130(5):677–9.
67. Haouchine B, Massin P, Tadayoni R, et al., Diagnosis of macular pseudoholes and lamellar macular holes by optical coherence tomography, *Am J Ophthalmol*, 2004;138(5):732–9.
68. Allen AW, Jr, Gass JD, Contraction of a perifoveal epiretinal membrane simulating a macular hole, *Am J Ophthalmol*, 1976;82(5):684–91.
69. Unoki N, Nishijima K, Kita M, et al., Lamellar Macular Hole Formation in Patients with Diabetic Cystoid Macular Edema, *Retina*, 2009;29(8):1128–33.
70. Hee MR, Puliafito CA, Wong C, et al., Optical coherence tomography of macular holes, *Ophthalmology*, 1995;102(5):748–56.
71. Ullrich S, Haritoglou C, Gass C, et al., Macular hole size as a prognostic factor in macular hole surgery, *Br J Ophthalmol*, 2002;86(4):390–3.
72. Larsson J, Holm K, Lovestam-Adrian M, The presence of an operculum verified by optical coherence tomography and other prognostic factors in macular hole surgery, *Acta Ophthalmol Scand*, 2006;84(3):301–4.
73. Frangieh GT, Green WR, Engel HM, A histopathologic study of macular cysts and holes, *Retina*, 1981;1(4):311–36.
74. Funata M, Wendel RT, de la Cruz Z, Green WR, Clinicopathologic study of bilateral macular holes treated with pars plana vitrectomy and gas tamponade, *Retina*, 1992;12(4):289–98.